Hindawi Publishing Corporation
Journal of Nanotechnology
Volume 2016, Article ID 5404529, 8 pages
http://dx.doi.org/10.1155/2016/5404529

Research Article

Antimicrobial Properties of Chitosan-Alumina/f-MWCNT Nanocomposites

Monaheng Masheane,[1,2] Lebea Nthunya,[1,2] Soraya Malinga,[1] Edward Nxumalo,[2] Tobias Barnard,[3] and Sabelo Mhlanga[2]

[1]*Department of Applied Chemistry and the DST/Mintek Nanotechnology Innovation Centre-Water Research Node, University of Johannesburg, P.O. Box 17011, Doornfontein, Johannesburg 2028, South Africa*
[2]*Nanotechnology and Water Sustainability Research Unit, College of Science, Engineering and Technology, University of South Africa, Florida, Johannesburg 1709, South Africa*
[3]*Water and Health Research Centre, University of Johannesburg, P.O. Box 17011, Doornfontein, Johannesburg 2028, South Africa*

Correspondence should be addressed to Sabelo Mhlanga; mhlansd@unisa.ac.za

Received 27 June 2016; Accepted 18 October 2016

Academic Editor: Dmitriy A. Dikin

Antimicrobial chitosan-alumina/functionalized-multiwalled carbon nanotube (f-MWCNT) nanocomposites were prepared by a simple phase inversion method. Scanning electron microscopy (SEM) analyses showed the change in the internal morphology of the composites and energy dispersive spectroscopy (EDS) confirmed the presence of alumina and f-MWCNTs in the chitosan polymer matrix. Fourier transform infrared (FTIR) spectroscopy showed the appearance of new functional groups from both alumina and f-MWCNTs, and thermogravimetric analysis (TGA) revealed that the addition of alumina and f-MWCNTs improved the thermal stability of the chitosan polymer. The presence of alumina and f-MWCNTs in the polymer matrix was found to improve the thermal stability and reduced the solubility of chitosan polymer. The prepared chitosan-alumina/f-MWCNT nanocomposites showed inhibition of twelve strains of bacterial strains that were tested. Thus, the nanocomposites show a potential for use as a biocide in water treatment for the removal of bacteria at different environmental conditions.

1. Introduction

Safe drinking water is still a dream for many South African rural settlements. Polluted water threatens political, economic, and social life for humanity; it is also an affront to human self-esteem [1]. It is well known that the health of the communities is significantly affected by the quality of drinking water [2]. Some water sources in South Africa rural areas are polluted by microbial pathogens derived from human or livestock wastes. Poor sanitation and poor maintenance of water supply systems also contribute a major role in the degradation of water sources by the microbes [3]. The impact of waterborne diseases is substantial in South Africa, with an estimated 43000 deaths and over a million incidents of illness reported annually [4, 5]. The diseases mainly affect people with unfledged or compromised immune systems and in particular young and elderly people and those living with HIV/AIDS [2].

Many conventional methods used in water treatment such as disinfection using chlorine have been used. However, these are known to produce disinfection by products (DBPs) which are of environmental concern [6]. Chitosan, which is a linear polysaccharide composed of randomly distributed β-(1–4)-linked D-glucosamine and N-acetyl-D-glucosamine (Figure 1), has a potential use in drinking water disinfection, as an antimicrobial agent in membranes, as an adsorbent (beads, sponges), and as a coating for water storage tanks [7–9]. Furthermore, it has advantages over other disinfection materials since it is has high antimicrobial activities with lower toxicity to humans and animals. Chitosan is also

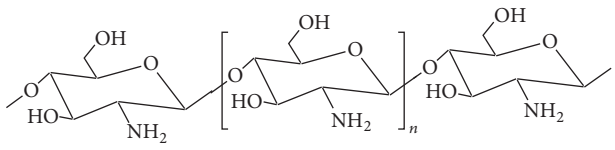

Figure 1: Structure of a chitosan polymer.

a bioactive and biocompatible material which is rendered useful in many applications including wound dressing, pharmaceutical and cosmetic products, and water treatment [10, 11].

The antimicrobial activities of chitosan are due to its polycationic nature. These result from the electrostatic interaction between the positively charged amine groups of chitosan and the negatively charged cell membrane of the microbes [12]. This electrostatic interaction results in a two-fold interference: (i) by promoting changes in the properties of membrane wall permeability, thus provoking internal osmotic imbalances, and (ii) consequently inhibiting the growth of microorganisms [13, 14]. Secondly, the hydrolysis of the peptidoglycans in the microorganism wall leads to the leakage of intracellular electrolytes such as potassium ions and other low molecular weight proteinaceous constituents (e.g., proteins, nucleic acids, glucose, and lactate dehydrogenase) [15–17]. This suggests that the higher the number of cationized amines, the higher the antimicrobial activity [18]. The third mechanism of antimicrobial activities is the binding bacterial DNA and inhabitation of mRNA synthesis which occur via penetration of chitosan into the nuclei of the microorganisms thereby interfering with the synthesis of mRNA and proteins resulting in the death of these organisms [19, 20]. Finally, the chelation of metals, suppression of spore elements, and binding to essential nutrients to microbial growth lead to cell death [21].

Although chitosan has been proven to have antimicrobial properties, its applications are limited due to factors such as water solubility and working pH [19, 22]. Cross-linkers such as epichlorohydrin and glutaraldehyde and inorganic materials such as alumina, silica, and titania have been used to improve its chemical stability [23]. The well-known characteristics of alumina as adsorbents are due to its high surface area (~200 m^2/g) and its amphoteric character of hydrous aluminum hydroxide. Its acid-based dissociation leads to the positive (OH^{2+}) at lower pH [24, 25]. Multiwalled carbon nanotubes (MWCNTs) have also become ideal materials to use as inorganic fillers for reinforcing or toughening polymeric materials [26]. Given its favorable attributes as discussed above, this study investigated chitosan and its nanostructured composites in the removal of microbes from water. The synthesis of chitosan/alumina composites embedded with functionalized MWCNTs (f-MWCNTs) has not been reported by others. The materials demonstrated antimicrobial activity on twelve strains of bacteria.

2. Experimental

2.1. Materials. Chitosan, alumina (particle size range: 30–60 nm), sodium hydroxide (NaOH), oxalic acid, iron (III) chloride hexahydrate ($FeCl_3 \cdot 6H_2O$), cobalt nitrate ($Co(NO_3)_2$), calcium carbonate ($CaCO_3$), sulphuric acid (H_2SO_4), nitric acid (HNO_3), and *p*-iodonitrotetrazolium chloride (INT) used in this study were supplied by Sigma Aldrich (Germany) and were used as received. The bacterial strains were obtained from the American Type Culture Collection (ATCC). MWCNTs were synthesized in our laboratory following a procedure by Mhlanga and Coville [27] and Mhlanga et al. [28]. Deionized water was obtained from a water purification system (Po process Ecopure GII Scientific) available in our laboratories.

2.2. Preparation of Chitosan/Alumina Composites. Chitosan/alumina gel (4 : 1 ratio of chitosan : alumina) was prepared by chelating alumina and chitosan using oxalic acid using a modified procedure reported by Li et al. [29] (Figure 2). Alumina was oxidized with 10% oxalic acid as a surface coating and then was washed with deionized water to pH = 7. The product was dried in an oven at 110°C overnight. The oxidized alumina powder was added to 2% chitosan gel prepared by a modified method reported by Ngah and Fatinathan [30] and Chatterjee and Woo [31]. The mixture was stirred for 12 h and then degassed.

2.3. Preparation of Chitosan-Alumina/f-MWCNT Nanocomposites. Chitosan-alumina/f-MWCNT nanocomposites (3.75 : 1 : 0.25) were prepared by adding a calculated amount of f-MWCNTs into a solution of chitosan-alumina prepared as described in Section 2.2 [29]. The mixture was stirred until being homogeneous and then degassed. The nanocomposite gel was then precipitated and then dried at 60°C in an oven. The illustration of the formation of chitosan-alumina/f-MWCNT nanocomposites is shown in Figure 2. Oxalic acid acts as a cross-linking agent between chitosan, alumina, and f-MWCNTs, thus forming a hydrogen bonding.

2.4. Antimicrobial Activity of the Nanocomposites. The bacterial strains shown in Table 1 were used to evaluate the antimicrobial properties of the chitosan and chitosan-alumina/f-MWCNT nanocomposites. The strains were plated and maintained on a Muller-Hinton agar (Oxoid, Cat. number CM0337) during the experiment. The plates were incubated at 37°C overnight and stored at 4°C. The bacterial strains were grown in liquid culture by inoculating Muller-Hinton broth (HI Media, Cat. number M391-500G) with a colony from the grown plates. All the liquid media were grown at 37°C with mild agitation (100 fpm) until an optimal density at 600 nm (OD_{600}) of 0.6 was reached. These cell suspensions, in media, were used in subsequent experiments.

All tests for antimicrobial activity of the nanocomposites were performed in a sterile 96-well micro titre plates with lids (NUNC microwell 96F, Cat. number 167008) and a single plate was used to test chitosan and chitosan-alumina/f-MWCNT nanocomposites against specific selected bacterial strains [32]. Sterile distilled water (50 μL) was added to each of the wells after which 50 μL of 2 μg/L test solution (chitosan and chitosan-based nanocomposites in water) was added to the first well, mixed, and transferred to the next well. The

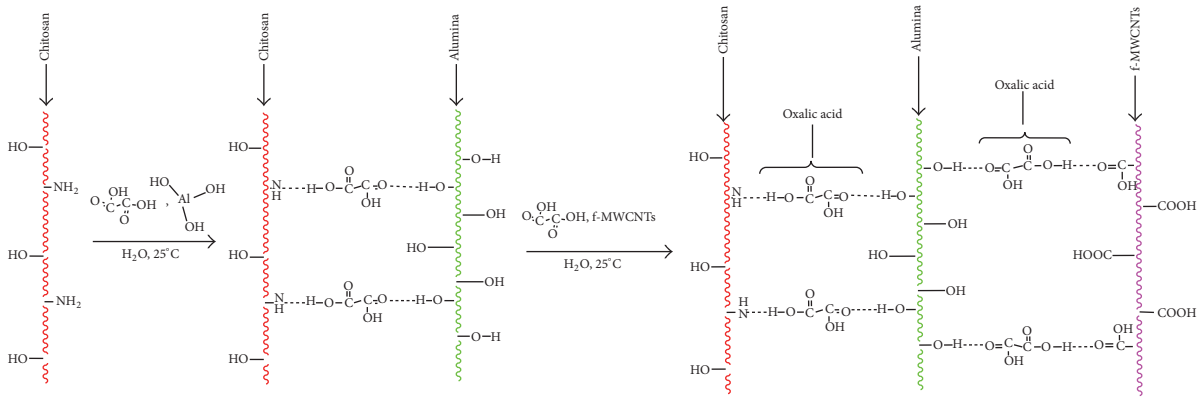

Figure 2: A schematic representation of the formation of chitosan-alumina/f-MWCNT nanocomposites.

Table 1: Summary of bacterial strains used for the testing of the nanocomposites.

Organism	ATCC number	Gram stain	Motility
Escherichia coli	259922	Gram negative	Motile
Escherichia coli	11775	Gram negative	Motile
Klebsiella pneumoniae	13882	Gram negative	Nonmotile
Klebsiella pneumoniae	31488	Gram negative	Nonmotile
Klebsiellla oxytoca	8724	Gram negative	Nonmotile
Pseudomonas aeruginosa	27853	Gram negative	Motile
Proteus mirabilis	12453	Gram negative	Motile
Shigella sonnei	25931	Gram negative	Nonmotile
Shigella boydii	9207	Gram negative	Nonmotile
Enterococcus faecalis	7080	Gram positive	Motile
Bacillus cereus	10876	Gram positive	Motile
Enterobacter cloacae	13047	Gram negative	Motile

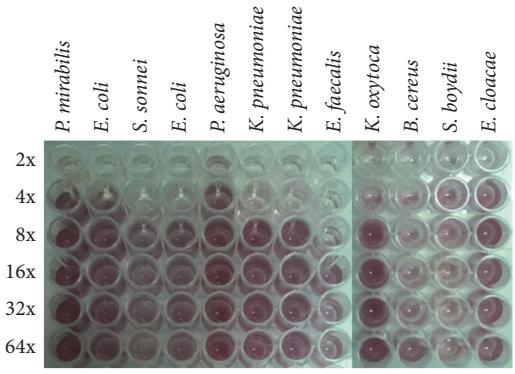

Figure 3: Example of a typical 96-well micro titre plate layout used for testing the nanocomposites. The clear wells show inhibition of bacterial growth and the purple wells indicate active cells reducing the INT.

serial dilutions were continued for 4 more times until the middle of the plate was reached after which the process was started again. To this, the bacterial cultures (50 μL) prepared as mentioned earlier were added to obtain the experimental setup shown in Figure 3. The micro titre plates were incubated overnight at 37°C. To indicate bacterial growth, 50 μL of INT dissolved in water were added to the micro plate wells and incubated at 37°C for 30 min. Active bacterial cells reduced the INT to produce a purple colour indicating bacterial survival, that is, no inhibition [32].

3. Results and Discussion

3.1. Morphology of Nanocomposites. Figure 4 shows SEM images and EDS spectra of chitosan, chitosan-alumina, and chitosan-alumina/f-MWCNT nanocomposites. A change in the internal morphology of chitosan after the incorporation of alumina and alumina/f-MWCNTs was observed. EDS confirmed that alumina and f-MWCNTs were included into the chitosan polymer matrix. This was evident by the presence of aluminum (Al), carbon (C), nitrogen (N), and oxygen (O) peaks detected on the EDS spectra of chitosan-alumina and chitosan-alumina/f-MWCNTs as shown in Figures 4(b) and 4(c).

3.2. FTIR Spectroscopy Analysis of Chitosan and Chitosan-Alumina/f-MWCNT Nanocomposites. The FTIR spectra of chitosan, chitosan-alumina, and chitosan-alumina/f-MWCNT nanocomposites are shown in Figure 5. In the spectrum of chitosan, the following characteristic adsorption

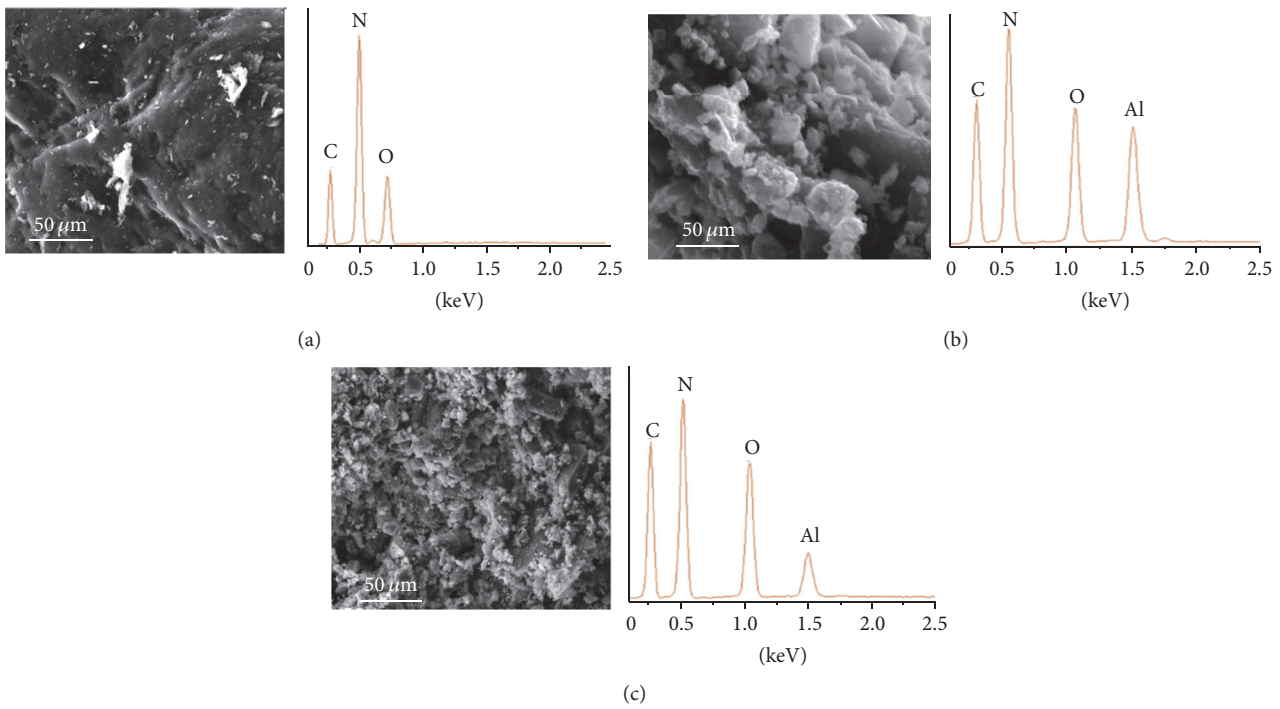

Figure 4: The SEM images and corresponding EDS spectra of chitosan (a), chitosan-alumina (b), and chitosan-alumina/f-MWCNTs (c).

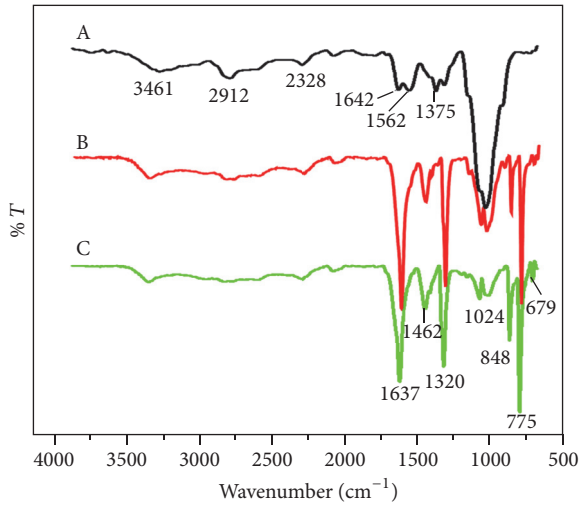

Figure 5: FTIR spectra of chitosan (A), chitosan-alumina (B), and chitosan-alumina/f-MWCNTs (C).

bands were observed: -OH and -NH_2 stretching vibrations (3461 cm^{-1}), the -CH stretching vibrations in -CH and -CH_2, (2912 cm^{-1}) the -C-C- stretching vibrations (2328 cm^{-1}), the -C=O stretching vibration in acetyl group (1642 cm^{-1}), the -NH_2 band vibration (1562 cm^{-1}), the -C-N stretching vibration in R_1R_2-$CHNH_2$ (1375 cm^{-1}), and -CO stretching in -COH (1024 cm^{-1}).

After addition of the alumina and f-MWCNTs, a surface interaction between chitosan and Al occurred and resulted in new peaks. The bands in the range of 1000–500 cm^{-1} were characteristics of aluminum oxide [33]. The peaks at 775 and 679 cm^{-1} were assigned to the Al-O stretching mode and bending mode of O-Al-O, respectively. In addition to the characteristic peaks of Al, there were new sharp peaks at 1637, 1462, and 1320 cm^{-1}, which represented the O-C=O bending vibration of oxalic acid, C-O and C-C stretching vibration, and the C=O asymmetric stretching vibration, respectively. The peaks present in the chitosan-alumina spectrum were still present in the spectrum of chitosan-alumina/f-MWCNTs. The only notable peak in spectrum of chitosan-alumina/f-MWCNTs was at 2912 cm^{-1} which was due to -C-H stretching vibrations. This suggested that there was a chemical interaction between chitosan, alumina, MWCNTs, and oxalic acid [29].

3.3. Thermal Analysis of Chitosan and Chitosan-Based Nanocomposites. The thermograms and derivative weight plots of chitosan and chitosan-alumina/f-MWCNTs are presented in Figure 6. It was observed that chitosan lost its mass in two steps. The first step mass loss (i) in Figure 6(a) occurred in the range of 50–130°C. This first mass loss step was ascribed to the loss of water molecules since the polysaccharides normally have strong affinity for water and thus are easily hydrated. The second step mass loss started at 280°C and reached the maximum at 620°C corresponding to the thermal and oxidative decomposition of chitosan [34, 35]. Specifically, the degradation involved decomposition of amine groups (ii) and polymer chain degradation (iii) in Figure 6(a).

The chitosan-alumina thermogram demonstrated an additional mass loss (iv) observed at 710°C (Figure 6(b)). This mass loss was due to the dehydroxylation of Al_2O_3 [36].

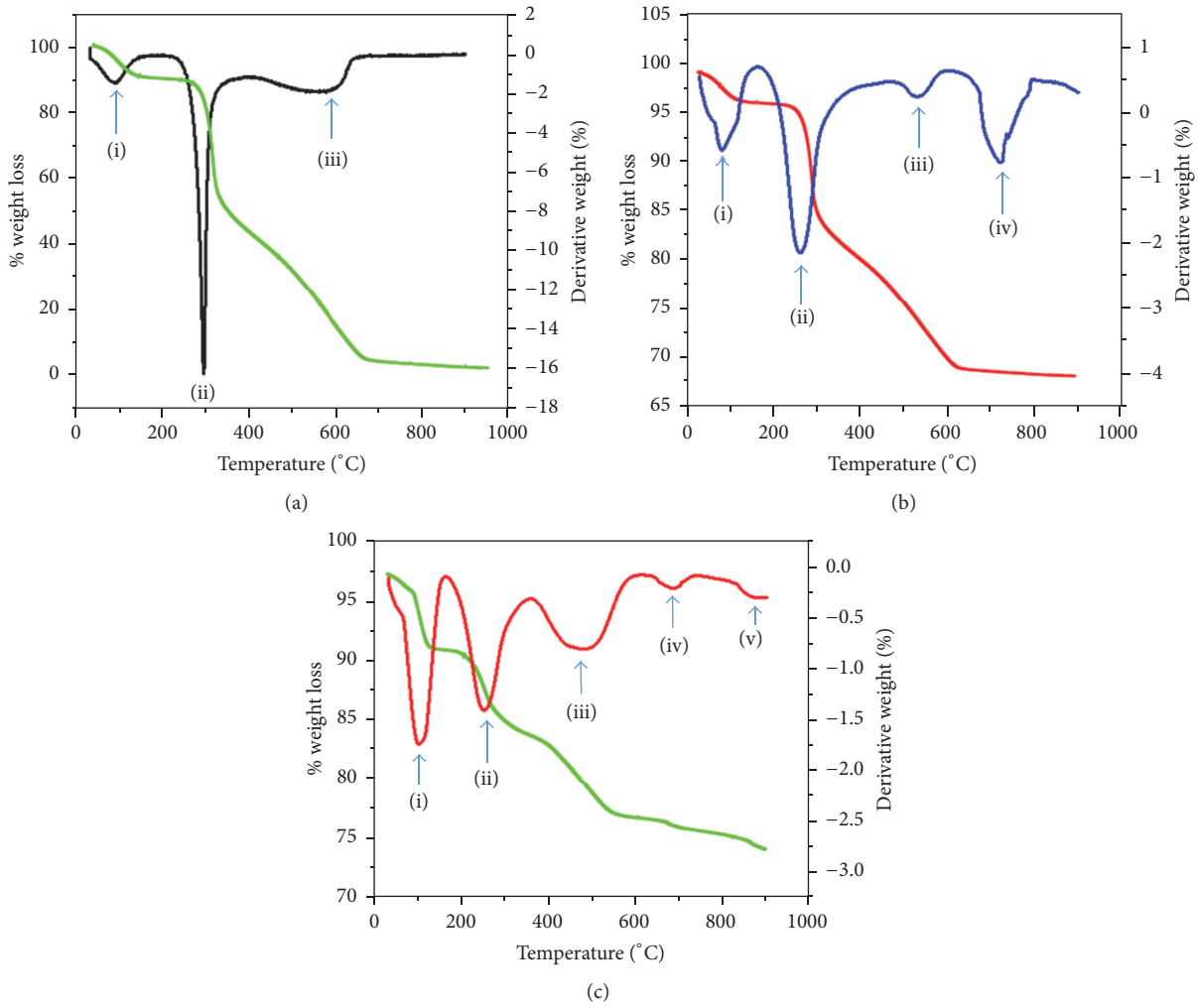

Figure 6: TGA and TGA derivative curves of chitosan (a), chitosan-alumina (b), and chitosan-alumina/f-MWCNTs (c) nanocomposites.

For chitosan-alumina/f-MWCNT nanocomposite, there was also an additional mass loss (v) in Figure 6(c) observed at 890°C, which was attributed to thermal degradation of MWCNTs. Generally, the addition of Al and f-MWCNTs to chitosan polymer matrix increased the thermal stability of the polymer. Basically, chitosan completely decomposed in air while chitosan-alumina and chitosan-alumina/f-MWCNTs decomposed to about 75%. The remaining mass corresponds to the amount of the alumina and f-MWCNTs added to the polymer matrix.

3.4. Solubility of Chitosan and Chitosan-Based Nanocomposites. The solubility of chitosan and chitosan-based nanocomposites is shown in Table 2. It was observed that chitosan composites were soluble in 0.1 M HAc (pH 3) solution but were insoluble in distilled water (pH = 7) and 0.1 M NaOH (pH = 9) solutions. Chitosan dissolved in acidic medium (pH 3) because the primary amino groups are protonated and this results in the degradation of the chitosan polymer chain. However, modification of chitosan with alumina and f-MWCNTs reduced their solubility. On the other hand, chitosan-alumina and chitosan-alumina/f-MWCNTs were found to be insoluble in all three media (Table 2). This was because there were fewer primary amino groups which can be protonated and cause dissolution by the cross-linker [37].

Table 2: Solubility effect of chitosan and chitosan-based nanocomposites.

Adsorbent	Solubility in solvents		
	0.1 M HAc	Distilled water	0.1 M NaOH
Chitosan	Soluble	Insoluble	Insoluble
Chitosan-alumina	Insoluble	Insoluble	Insoluble
Chitosan-alumina/f-MWCNTs	Insoluble	Insoluble	Insoluble

3.5. Antimicrobial Properties of the Nanocomposites. Figure 5 shows the antimicrobial effect of chitosan and chitosan-based

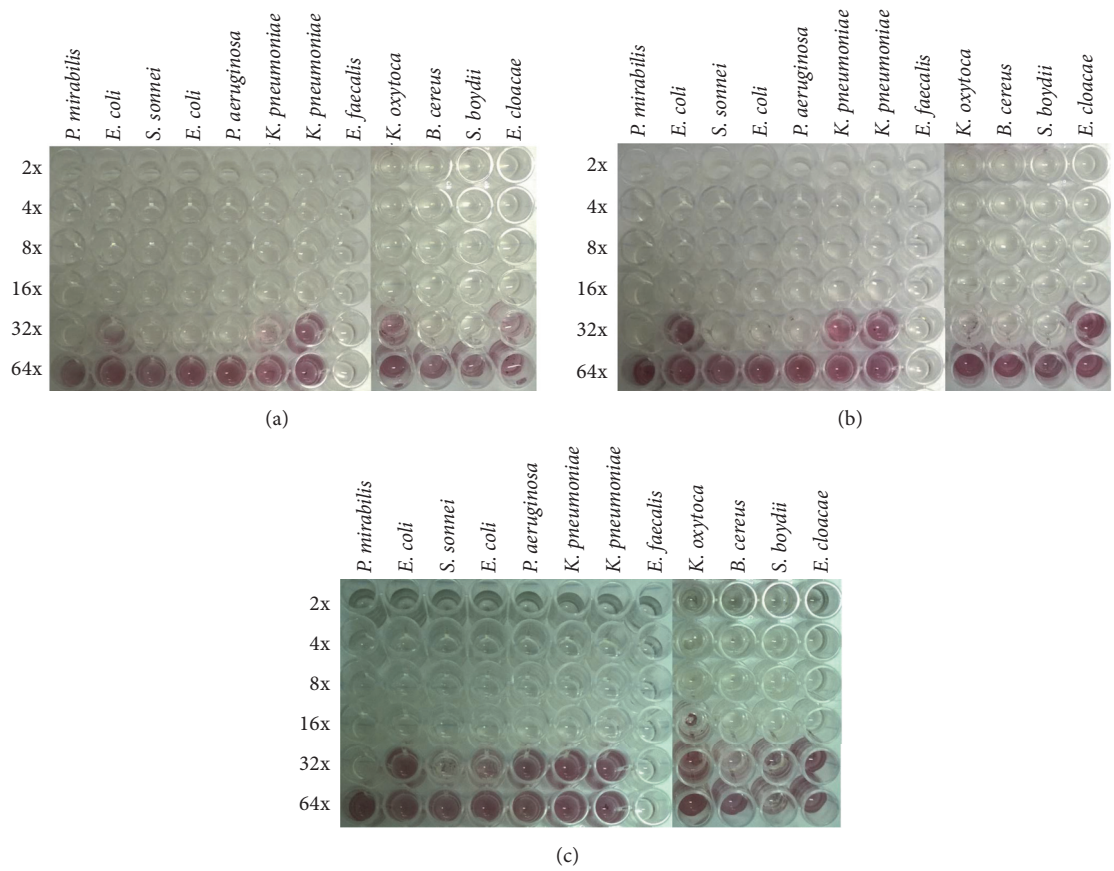

Figure 7: The antimicrobial effect of chitosan (a), chitosan-alumina (b), and chitosan-alumina/f-MWCNTs (c) on various strains of bacteria. Clear wells indicated that there was no growth/inhibition of the bacteria. Purple wells indicate growth (no inhibition) of the bacteria.

nanocomposites. All the nanocomposites (initial concentration = 2 mg/mL, i.e., 2 mg of beads in 1 mL of water) showed some growth inhibition to all bacterial strains. Typically, all the beads demonstrated complete (100%) inhibition at all concentrations (from high, i.e., 1 mg/mL = 2x, dilution in Figures 7(a), 7(b), and 7(c) to low, that is, 31.25 μg/mL = 64x, dilution in Figures 7(a), 7(b), and 7(c)) for *E. faecalis* bacterial strains. However, further dilution needed to be done in order to determine the minimum inhibition concentration (MIC) for *E. faecalis*. The MIC of the nanocomposites for other bacterial strains other than *E. faecalis* was in the range of 62.5 μg/mL–0.25 mg/L (Table 3). The antimicrobial activity of the nanocomposites was attributed to the positively charged active sites (-NH_2 and -OH groups in acidic media) of the materials, which interact with the negatively charged cell wall of the bacterial strains, thus causing the death of the bacteria.

Table 3: Summary of the highest dilutions (MICs) of the beads that inhibited the bacterial growth as determined by the INT assay.

Organism	Nanocomposites (μg/L)		
	Chitosan	Chitosan-alumina	Chitosan-alumina/f-MWCNTs
E. faecalis	Up to 31.3	Up to 31.3	Up to 31.3
K. pneumoniae	125	125	125
K. pneumoniae	125	125	125
P. aeruginosa	62.5	62.5	125
E. coli	62.5	62.5	125
S. sonnei	62.5	62.5	125
E. coli	125	125	125
P. mirabilis	62.5	62.5	62.5
K. oxytoca	125	125	125
B. cereus	62.5	62.5	125
S. boydii	62.5	62.5	125
E. cloacae	125	125	250

4. Conclusions

Chitosan-alumina/f-MWCNT nanocomposites with antimicrobial properties were prepared by a simple phase inversion using oxalic acid as a cross-linker. The incorporation of alumina and f-MWCNTs on chitosan improved the thermal stability and reduced the solubility and swelling behaviour of chitosan. The chitosan-alumina/f-MWCNT nanocomposites showed similar antimicrobial activity as pristine chitosan; however, their physicochemical properties such as thermal stability and lower solubility were improved properties.

Therefore, the novel chitosan-alumina/f-MWCNT nanocomposites could be used as antimicrobial agents even at lower pH and high temperatures without any degradation.

Competing Interests

The authors declare that there is no conflict of interests regarding the publication of this paper.

Acknowledgments

The authors wish to thank DST/NRF Nanotechnology Flagship Project (Grant no. 97823), the Water Research Commission, DST/Mintek Nanotechnology Innovation Centre (NIC), Water and Health Research Centre (University of Johannesburg), and the University of South Africa for supporting this work.

References

[1] World Health Organization, *Emerging Issues in Water and Infectious Disease*, World Health Organization, Geneva, Switzerland, 2003.

[2] B. Momba, N. Makala, and R. Kelly, "Possible threat of the microbiological and chemical contamination of the Mpofu Training Centre borehole to the health of the surrounding community," in *Proceedings of the WISA Conference*, pp. 1–7, 2008.

[3] U. Singh, R. Lutchmanariayan, J. Wright et al., "Microbial quality of drinking water from groundtanks, standpipes and community tankers at source and point of use in Ethekwini Municipality, and its relationship to health outcomes," *Water SA*, vol. 39, no. 5, pp. 1–22, 2013.

[4] L. N. Nthunya, M. L. Masheane, S. P. Malinga et al., "UV-assisted reduction of *in situ* electrospun antibacterial chitosan-based nanofibres for removal of bacteria from water," *RSC Advances*, vol. 6, no. 98, pp. 95936–95943, 2016.

[5] G. C. Pegram, N. Rollins, and Q. Espey, "Estimating the costs of diarrhoea and epidemic dysentery in KwaZulu-Natal and South Africa," *Water SA*, vol. 24, no. 1, pp. 11–20, 1998.

[6] B. An, K.-Y. Jung, S.-H. Lee, S. Lee, and J.-W. Choi, "Effective phosphate removal from synthesized wastewater using copper-chitosan bead: batch and fixed-bed column studies," *Water, Air, & Soil Pollution*, vol. 225, no. 8, pp. 2050–2062, 2014.

[7] P. K. Dutta, V. S. Tripathi, G. K. Mehrotra, and J. Dutta, "Perspectives for chitosan based antimicrobial films in food applications," *Food Chemistry*, vol. 114, no. 4, pp. 1173–1182, 2009.

[8] J. Dutta, V. S. Tripathi, and P. K. Dutta, "Progress in antimicrobial activities of chitin, chitosan and its oligosaccharides: a systematic study needs for food applications," *Food Science and Technology International*, vol. 18, no. 1, pp. 3–34, 2012.

[9] R. Rajendran, M. Abirami, P. Prabhavathi, P. Premasudha, B. Kanimozhi, and A. Manikandan, "Biological treatment of drinking water by chitosan based nanocomposites," *African Journal of Biotechnology*, vol. 14, no. 11, pp. 930–936, 2015.

[10] P. K. Dutta, J. Duta, and V. S. Tripathi, "Chitin and chitosan: chemistry, properties and applications," *Journal of Scientific and Industrial Research*, vol. 63, no. 1, pp. 20–31, 2004.

[11] L. S. Abebe, X. Chen, and M. D. Sobsey, "Chitosan coagulation to improve microbial and turbidity removal by ceramic water filtration for household drinking water treatment," *International Journal of Environmental Research and Public Health*, vol. 13, no. 3, pp. 1–8, 2016.

[12] S. Tripathi, G. K. Mehrotrap, and P. K. Dutta, "Preparation and antimicrobial activity of chitosan-silver oxide nanocomposite film via solution casting method," *Bulletin of Materials Science*, vol. 34, no. 1, pp. 29–35, 2011.

[13] L. A. Hadwiger, D. Kendra, B. W. Fristensky, and W. Wagoner, "Chitosan both activates genes in plants and inhibits RNA synthesis in fungi," in *Chitin in Nature and Technology*, pp. 209–214, 2016.

[14] F. Shahidi, J. K. V. Arachchi, and Y.-J. Jeon, "Food applications of chitin and chitosans," *Trends in Food Science and Technology*, vol. 10, no. 2, pp. 37–51, 1999.

[15] M. A. Papineau, G. D. Hoover, D. Knorr, and F. D. Farkas, "Antimicrobial effect of water–soluble chitosans with high hydrostatic pressure," *Food Biotechnology*, vol. 5, no. 1, pp. 45–57, 1991.

[16] C.-S. Chen, W.-Y. Liau, and G.-J. Tsai, "Antibacterial effects of N-sulfonated and N-sulfobenzoyl chitosan and application to oyster preservation," *Journal of Food Protection*, vol. 61, no. 9, pp. 1124–1128, 1998.

[17] W. F. Shao, F. L. Chin, and S. Daniel, "Antifungal activity of chitosan and its preservative effect on low sugar candied Kumquat," *Journal of Food Protection*, vol. 57, no. 2, pp. 136–140, 1994.

[18] M. Másson, J. Holappa, M. Hjálmarsdóttir, Ö. V. Rúnarsson, T. Nevalainen, and T. Järvinen, "Antimicrobial activity of piperazine derivatives of chitosan," *Carbohydrate Polymers*, vol. 74, no. 3, pp. 566–571, 2008.

[19] S. Chen, G. Wu, D. Long, and Y. Liu, "Preparation, characterization and antibacterial activity of chitosan-$Ca_3V_{10}O_{28}$ complex membrane," *Carbohydrate Polymers*, vol. 64, no. 1, pp. 92–97, 2006.

[20] R. C. Goy, D. de Britto, and O. B. G. Assis, "A review of the antimicrobial activity of chitosan," *Polímeros: Ciência e Tecnologia*, vol. 19, no. 3, pp. 241–247, 2009.

[21] G. Mario, D. Raul, P. Felicidad, B. Tatiana, G. Juan, and G. Iris, "Influence of chitosan addition on quality properties of vacuum packaged pork sausages Influência da adição de quitosana sobre a qualidade de," *Food Science and Technology*, vol. 30, no. 2, pp. 1–7, 2016.

[22] S. K. Yadav, S. S. Mahapatra, M. K. Yadav, and P. K. Dutta, "Mechanically robust biocomposite films of chitosan grafted carbon nanotubes via the [2 + 1] cycloaddition of nitrenes," *RSC Advances*, vol. 3, no. 45, pp. 23631–23637, 2013.

[23] F.-L. Mi, S.-J. Wu, and F.-M. Lin, "Adsorption of copper(II) ions by a chitosan-oxalate complex biosorbent," *International Journal of Biological Macromolecules*, vol. 72, pp. 136–144, 2015.

[24] K. Azlan, W. N. Wan Saime, and L. Lai Ken, "Chitosan and chemically modified chitosan beads for acid dyes sorption," *Journal of Environmental Sciences*, vol. 21, no. 3, pp. 296–302, 2009.

[25] A. K. Khattak, M. Afzal, M. Saleem, G. Yasmeen, and R. Ahmad, "Surface modification of alumina by metal doping," *Colloids and Surfaces A*, vol. 162, no. 1–3, pp. 99–106, 2000.

[26] S. C. Tjong, "Structural and mechanical properties of polymer nanocomposites," *Materials Science and Engineering: R: Reports*, vol. 53, no. 3-4, pp. 73–197, 2006.

[27] S. D. Mhlanga and N. J. Coville, "Iron-cobalt catalysts synthesized by a reverse micelle impregnation method for controlled

growth of carbon nanotubes," *Diamond and Related Materials*, vol. 17, no. 7–10, pp. 1489–1493, 2008.

[28] S. D. Mhlanga, K. C. Mondal, M. J. Witcomb, and N. J. Coville, "The effect of synthesis parameters on the catalytic synthesis of multiwalled carbon nanotubes using Fe–Co/$CaCO_3$ catalysts," *South African Journal of Chemistry*, vol. 62, pp. 67–76, 2009.

[29] W.-Y. Li, J. Liu, H. Chen et al., "Application of oxalic acid cross-linking activated alumina/chitosan biocomposites in defluoridation from aqueous solution. Investigation of adsorption mechanism," *Chemical Engineering Journal*, vol. 225, pp. 865–872, 2013.

[30] W. S. W. Ngah and S. Fatinathan, "Pb(II) biosorption using chitosan and chitosan derivatives beads: equilibrium, ion exchange and mechanism studies," *Journal of Environmental Sciences*, vol. 22, no. 3, pp. 338–346, 2010.

[31] S. Chatterjee and S. H. Woo, "The removal of nitrate from aqueous solutions by chitosan hydrogel beads," *Journal of Hazardous Materials*, vol. 164, no. 2-3, pp. 1012–1018, 2009.

[32] J. N. Eloff, "A sensitive and quick microplate method to determine the minimal inhibitory concentration of plant extracts for bacteria," *Planta Medica*, vol. 64, no. 8, pp. 711–713, 1998.

[33] S. Jagtap, M. K. N. Yenkie, N. Labhsetwar, and S. Rayalu, "Defluoridation of drinking water using chitosan based mesoporous alumina," *Microporous and Mesoporous Materials*, vol. 142, no. 2-3, pp. 454–463, 2011.

[34] N. M. El-Sawy, H. A. Abd El-Rehim, A. M. Elbarbary, and E.-S. A. Hegazy, "Radiation-induced degradation of chitosan for possible use as a growth promoter in agricultural purposes," *Carbohydrate Polymers*, vol. 79, no. 3, pp. 555–562, 2010.

[35] F. A. A. Sagheer, M. A. Al-Sughayer, S. Muslim, and M. Z. Elsabee, "Extraction and characterization of chitin and chitosan from marine sources in Arabian Gulf," *Carbohydrate Polymers*, vol. 77, no. 2, pp. 410–419, 2009.

[36] J. Li, X. Wang, L. Wang et al., "Preparation of alumina membrane from aluminium chloride," *Journal of Membrane Science*, vol. 275, no. 1-2, pp. 6–11, 2006.

[37] T. Jóźwiak, U. Filipkowska, P. Szymczyk, and A. Mielcarek, "Application of cross-linked chitosan for nitrate nitrogen (V) removal from aqueous solutions," *Progress on Chemistry and Application of Chitin and Its Derivatives*, vol. 19, no. 3, pp. 41–52, 2014.